Phytochemistry 162 (2019) 21–28

Contents lists available at ScienceDirect

Phytochemistry

journal homepage: www.elsevier.com/locate/phytochem

Triterpenes with unusual modifications from the fruiting bodies of the medicinal fungus *Irpex lacteus*

Yang Tang[a,b], Zhen-Zhu Zhao[b,c], Tao Feng[a], Zheng-Hui Li[a], He-Ping Chen[a,b,*], Ji-Kai Liu[a,b,**]

[a] School of Pharmaceutical Sciences, South-Central University for Nationalities, Wuhan, 430074, People's Republic of China
[b] State Key Laboratory of Phytochemistry and Plant Resources in West China, Kunming Institute of Botany, Chinese Academy of Sciences, Kunming, 650201, People's Republic of China
[c] College of Pharmacy, Henan University of Chinese Medicine, Zhengzhou, 450046, China

ARTICLE INFO

Keywords:
Irpex lacteus (Fr.) Fr.
Phanerochaetaceae
Eburicane
19(10 → 5)*abeo*-eburicane
Lanostane
Triterpenoids
Cytotoxicity

ABSTRACT

Ten previously undescribed triterpenoid congeners, namely irpeksolactins A–J, together with eighteen known ones, were isolated from the fruiting bodies of the rainforest-dwelling medicinal fungus *Irpex lacteus*. The structures of all the isolates were characterized by extensive spectroscopic approaches, including 1D & 2D NMR and MS spectroscopic methods. Irpeksolactin J displayed selective and weak cytotoxicity against the human lung cancer cell line A549 and the human hepatocellular carcinoma cell line SMMC-7721.

1. Introduction

The fungus *Irpex lacteus* (Fr.) Fr. is a wood decaying fungus belongs to the Family Phanerochaetaceae and is the type species of the genus *Irpex* (http://www.mycobank.org/BiolomicsDetails.aspx?Rec=58932). This fungus has long been used as folk medicine for treating oliguria, oedema, and hypertension. The polysaccharide fraction of this fungus has been developed as a drug used to cure glomerulonephritis clinically with the trade name Yishenkang (Dong et al., 2017). Beyond the pharmaceutical use, it is currently regarded as the most important lignocellulose-degrading organism due to its potential in lignin degradation and industrial pollutants cleaning (Cajthaml et al., 2008). Recently, the genome sequence of *I. lacteus* has been reported, which was considered to provide insights into the mechanisms of the efficient lignin decomposition of this strain (Yao et al., 2017).

Although nearly half-century's attention has been paid on macromolecules of this fungus, and have achieved a lot in the aspects of drug development and biotechnological utilization, however, merely a handful of literatures referred to its specialised metabolites. Chemical investigations on the specialised metabolites of the liquid cultures led to the reports of the nematicidal substances L-1, L-2, and L-3 (Hayashi et al., 1981), and the novel sesquiterpenoids irlactins A–D (Ding et al., 2013). Due to the difficulty to obtain enough fruiting bodies of *I. lacteus* for chemical study, no literature has focused on the constituents of its fruiting bodies until triterpenes irpeksins A–E (Tang et al., 2018b), and irpexoates A–D (Tang et al., 2018a) were reported. In a continuing program to discover promising natural products as drug leads from medicinal fungi and the deepgoing research on this fungus, herein, we report 28 triterpenes, including 10 previously undescribed ones which designated the name irpeksolactins A–J (**1–10**) (Fig. 1), isolated from the fruiting bodies of *I. lacteus*. In this paper, we will highlight the isolation, structural elucidation, and biological evaluation of these triterpenoids.

2. Results and discussion

2.1. Structure elucidation of previously undescribed triterpenes (1–10)

Compound **1** (Fig. 1) was obtained as white, amorphous powder. It gave a sodium adduct ion peak at *m/z* 523.3398 $[M + Na]^+$ in the (+)-HRESIMS analysis, indicating the molecular formula of $C_{31}H_{48}O_5$ (calcd for $C_{31}H_{48}O_5Na$, 523.3394). The ^1H NMR data (Table 1) showed resonances for five singlet methyls at δ_H 0.69 (Me-18), 1.14 (Me-29), 1.20 (Me-28), 1.28 (Me-30), 2.30 (Me-19), and two methyl doublets at δ_H 1.02 (d, J = 6.9 Hz, Me-26), 1.03 (d, J = 6.9 Hz, Me-27), two oxygenated methine protons at δ_H 3.47 (d, J = 10.0 Hz, H-3) and 4.27 (dd, J = 8.5, 6.5 Hz, H-16), and two mutually coupled aromatic protons at δ_H 6.96 (d, J = 7.7 Hz, H-6) and 6.77 (d, J = 7.7 Hz, H-7). The ^{13}C NMR

* Corresponding author.School of Pharmaceutical Sciences, South-Central University for Nationalities, Wuhan, 430074, People's Republic of China.
** Corresponding author.School of Pharmaceutical Sciences, South-Central University for Nationalities, Wuhan, 430074, People's Republic of China.
E-mail addresses: chenhp@mail.scuec.edu.cn (H.-P. Chen), jkliu@mail.kib.ac.cn, liujikai@mail.scuec.edu.cn (J.-K. Liu).

https://doi.org/10.1016/j.phytochem.2019.02.017
Received 7 November 2018; Received in revised form 24 February 2019; Accepted 27 February 2019
Available online 06 March 2019
0031-9422/

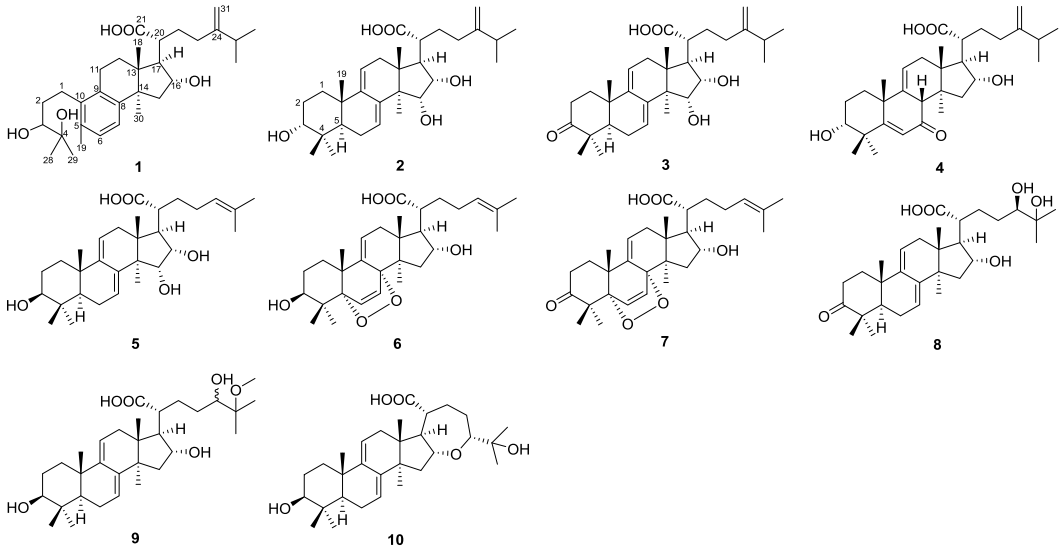

Fig. 1. Structures of compounds **1–10**.

Table 1
^{1}H NMR spectroscopic data for compounds **1–6**.

No.	1[a,d]	2[b,e]	3[b,d]	4[c,f]	5[c,e]
1	2.94, ddd (13.0, 13.0, 4.5)	1.80, overlapped	2.24, dd (13.0, 7.0)	2.63, ddd (13.0, 3.0, 4.0)	2.00, overlapped
	2.55, overlapped	1.68, overlapped	1.74, ddd (13.0, 13.0, 4.5)	1.57, d (13.0)	1.41, ddd (13.0, 13.0, 5.0)
2	1.55, m	2.00, overlapped	2.76, ddd (14.0, 14.0, 6.0)	2.23, br. dd (13.0, 13.0)	1.69, overlapped
	1.43, m	1.66, overlapped	2.35, ddd (14.6, 4.0, 4.0)	1.96, dd (13.0, 3.5)	1.66, overlapped
3	3.47, d (10.0)	3.38, br. t (3.0)		3.78, br. t (3.5)	3.16, dd (11.0, 5.0)
5		1.57, dd (11.0, 5.0)	1.54, dd (11.6, 4.0)		1.09, dd (11.7, 4.0)
6	6.96, d (7.7)	2.07, overlapped, 2H	2.18, overlapped	6.41, s	2.17, m
			2.14, dd (7.0, 4.0)		2.08, d (12.0)
7	6.77, d (7.7)	5.95, d (6.0)	5.99, d (6.0)		5.95, d (6.3)
11	2.87, ddd (17.0, 17.0, 9.0)	5.34, d (6.0)	5.35, d (6.0)	5.75, s	5.33, d (6.0)
	2.84, ddd (17.0, 9.0, 9.0)				
12	2.09, m	2.24, dd (17.0, 6.0)	2.28, d (18.0)	2.59, overlapped	2.22, d (17.0)
	1.70, dd (13.0, 8.5)	1.88, d (17.0)	1.84, dd (18.0, 6.4)	2.37, overlapped	1.84, d (17.0, 6.4)
15	2.46, dd (13.5, 8.5)	4.03, d (8.0)	4.12, d (7.0)	2.79, dd (13.0, 7.5)	4.02, d (8.0)
	1.82, d (13.5)			2.73, d (13.0)	
16	4.27, dd (8.5, 6.5)	3.80, dd (8.0, 6.0)	3.90, br. t (7.0)	4.52, dd (7.5, 7.5)	3.78, dd (8.0, 6.0)
17	2.31, dd (11.0, 6.5)	2.01,overlapped	2.10, dd (11.0, 7.0)	2.81, dd, (12.0, 7.5)	1.98, overlapped
18	0.69, s	0.68, s	0.68, s	1.22, s	0.66, s
19	2.30, s	1.01, s	1.18, s	1.43, s	0.99, s
20	2.52, m	2.38, td (12.0, 3.0)	2.49, dd (11.0, 3.5)	2.96, ddd (11.0, 11.0, 4.0)	2.36, ddd (11.5, 11.5, 3.0)
22	1.89, overlapped	2.08, overlapped	2.00, overlapped	2.70, overlapped	1.87, overlapped
	2.02, overlapped	2.01, overlapped	1.90, m	2.46, overlapped	1.68, overlapped
23	2.11,overlapped;	2.02, overlapped	2.11, overlapped	2.55, overlapped	2.02, overlapped
	2.03, overlapped	1.79, overlapped	2.02, m	2.43, overlapped	1.96, overlapped
24	2.25, m	2.27, m	2.23, overlapped	2.30, m	5.15, br. t (6.5)
26	1.03, d (6.9)	1.03, d (6.0)	1.03, d (7.0)	1.00, d (6.0)	1.60, s
27	1.02, d (6.9)	1.04, d (6.0)	1.02, d (7.0)	1.02, d (6.0)	1.68, s
28	1.20, s	0.96, s	1.09, s	1.39, s	0.99, s
29	1.14, s	0.94, s	1.12, s	1.20, s	0.87, s
30	1.28, s	0.92, s	0.93, s	1.32, s	0.90, s
31	4.78, s	4.77, s	4.79, s	5.01, s	
	4.73, s	4.75, s	4.73, s	4.87, s	

[a] Recorded at 800 MHz.
[b] Recorded at 600 MHz.
[c] Recorded at 500 MHz.
[d] Recorded in $CDCl_3$.
[e] Recorded in CD_3OD.
[f] Recorded in C_5D_5N.

and DEPT data (Table 3) presented carbon signals which were ascribable for seven methyls, seven methylenes, five sp^2-hybridized methines [two oxygenated ones at δ_C 77.2 (C-16) and 79.2 (C-3)], four pairs of double bonds, three sp^3-hybridized quaternary carbons (one oxygenated, δ_C 73.4 (C-4)), and a carboxylic acid group at δ_C 179.4 (C-21). The aforementioned data displayed high similarity to those of daedaleanic acid A, a 24-methyl lanostane (sometimes called eburicane) triterpenes isolated from the fruiting bodies of the fungus *Daedalea dickinsii* (Yoshikawa et al., 2005). The major structural discrepancies between **1** and daedaleanic acid A were that the substituted patterns of

Table 2
^{1}H NMR spectroscopic data for compounds **6–10** (CD_3OD).

No.	6[a]	7[b]	8[a]	9[b]	10[a]
1	1.91, overlapped	2.32, overlapped	2.36, overlapped	2.02, ddd (13.0, 4.0, 4.0)	2.02, ddd (13.0, 4.0, 4.0)
	1.66, overlapped	1.94, overlapped	1.71, dd (14.0, 14.0, 4.5)	1.42, ddd (13.0, 13.0, 5.0)	1.43, ddd (13.0, 13.0, 5.0)
2	1.73, overlapped	2.95, ddd (17.0, 17.0, 8.0)	2.85, ddd (14.0, 14.0, 6.0)	1.68, m	1.70, m
	1.76, overlapped	2.29, overlapped	2.29, ddd (14.0, 4.5, 3.0)	1.62, m	1.66, m
3	3.71, dd (11.0, 6.0)			3.16, dd (11.0, 4.5)	3.16, dd (10.0, 5.5)
5			1.55, dd (12.0, 4.0)	1.10, overlapped	1.10, dd (11.0, 7.0)
6	6.54, d (9.0)	6.60, d (9.0)	2.25, overlapped	2.14, overlapped	2.12, overlapped
			2.11, ddd (17.0, 7.0, 3.6)	2.08, overlapped	1.97, overlapped
7	6.80, d (9.0)	6.90, d (9.0)	5.55, d (6.5)	5.50, d (6.0)	5.50, d (6.0)
11	5.42, d (6.0)	5.54, d (6.0)	5.45, d (6.0)	5.35, d (6.0)	5.36, d (6.0)
12	2.23, d (17.0)	2.25, d (17.6)	2.28, br. d (17.0)	2.23, overlapped	2.35, d (18.0)
	1.79, overlapped	1.85, dd (17.6, 6.0)	1.90, dd (17.0, 6.5)	1.86, dd (18.0, 6.5)	1.93, overlapped
15	2.56, dd (14.0, 8.6)	2.57, dd (14.0, 8.6)	2.21, overlapped	2.18, overlapped	2.20, dd (13.8, 8.2)
	1.37, d (14.0)	1.37, d (14.0)	1.49, d (13.5)	1.48, d (13.5)	1.49, d (13.8)
16	4.11, t-like (7.0)	4.12, dd (7.4, 7.4)	4.11, dd (9.0, 6.0)	4.08, dd (8.2, 6.5)	4.18, t (7.5)
17	2.27, dd (11.0, 6.0)	2.28, overlapped	2.16, dd (12.0, 6.0)	2.14, overlapped	2.43, dd (10.0, 7.0)
18	0.85, s	0.89, s	0.66, s	0.63, s	0.62, s
19	1.17, s	1.40, s	1.21, s	0.99, s	0.99, s
20	2.40, ddd (11.0, 11.0, 3.2)	2.40, dd (11.0, 11.0)	2.37, overlapped	2.34, ddd (10.5, 10.5, 3.0)	2.73, ddd (8.5, 8.5, 7.0)
22	2.06, ddd (13.0, 13.0, 5.0)	1.89, overlapped	2.22, overlapped	2.21, m	2.18, overlapped
	1.64, overlapped	1.65, overlapped	1.59, overlapped	1.58, m	1.98, overlapped
23	2.02, overlapped	2.03, m	1.64, dd (16.0, 4.0)	1.34, m	1.95, overlapped
	1.94, overlapped	1.96, overlapped	1.26, m	1.25, m	1.91, overlapped
24	5.14, t (6.4)	5.15, t (7.0)	3.25, d (10.0)	3.37, d (10.0)	4.25, dd (10.8, 5.0)
26	1.60, s	1.61, s	1.12, s	1.13, s	1.24, s
27	1.68, s	1.68, s	1.15, s	1.09, s	1.23, s
28	1.07, s	1.42, s	1.07, s	0.99, s	0.99, s
29	1.13, s	1.07, s	1.14, s	0.88, s	0.88, s
30	1.15, s	1.15, s	1.10, s	1.08, s	1.12, s
-OMe				3.20, s	

[a] Recorded at 500 MHz.
[b] Recorded at 600 MHz.

C-3 and C-4. Only C-3 of daedaleanic acid A was oxygenated into a carbonyl group while both C-3 and C-4 of **1** were substituted by hydroxy groups, which were corroborated by HMBC correlations from Me-28 and Me-29 to C-3 and C-4 (Fig. 2). 16-OH was determined as *α* orientation by the key ROESY cross peaks between Me-18 and H-16 (δ_H 4.27) (Fig. 3). However, the absolute configuration of C-3 remained unassigned due to the shortage of samples to preparation of corresponding chemical derivatives. Thus, the structure of compound **1** was established as 3,4,16*α*-trihydroxy-19 (10 → 5)*abeo*-eburica-5,7,9-trien-21-oic acid (Fig. 1), and was named as irpeksolactin A.

The molecular formula of the white powder compound **2** was determined as $C_{31}H_{48}O_5$ by HRESIMS protonated ion peak at *m/z* 501.3572 $[M + H]^+$ (calcd for $C_{31}H_{49}O_5$, 501.3575), requiring eight degrees of unsaturation. The ^{1}H NMR data (Table 1) showed five methyl singlets at δ_H 0.68 (Me-18), 1.01 (Me-19), 0.96 (Me-28), 0.94 (Me-29), 0.92 (Me-30), two methyl doublets at δ_H 1.03 (d, J = 6.0 Hz, Me-26), and 1.04 (d, J = 6.0 Hz, Me-27), three oxygen-bearing methine protons at δ_H 3.38 (br. t, J = 3.0 Hz, H-3), 4.03 (d, J = 8.0 Hz, H-15), and 3.80 (dd, J = 8.0,6.0 Hz, H-16), an olefinic methylene at δ_H 4.75 (s, H-31a) and 4.77 (s, H-31b), and two olefinic methines at δ_H 5.95 (d, J = 6.0 Hz, H-7) and 5.34 (d, J = 6.0 Hz, H-11). The ^{13}C NMR data (Table 3) exhibited 31 carbon resonances which were classified into a carboxylic group at δ_C 180.5 (C-21), six olefinic carbons at δ_C 123.1 (C-7), 142.3 (C-8), 147.9 (C-9), 116.4 (C-11), 156.9 (C-24), 107.5 (C-31), and three oxygenated methines carbons at δ_C 76.9 (C-3), 74.0 (C-15) and 76.1 (C-16). The data showed great resemblance to those of 15*α*-hydroxydehydrotumulosic acid (Akihisa et al., 2007), an eburicane-type triterpene obtained from the medicinal fungus *Poria cocos*. Analysis of the ^{1}H–^{1}H COSY and HMBC data of **2** enabled the completion of its planar structure as shown in Fig. 2, which was established to be consistent with that of 15*α*-hydroxydehydrotumulosic acid. Analysis of the coupling constants of the ^{1}H NMR and ROESY spectra indicated that the only difference between **2** and 15*α*-hydroxydehydrotumulosic acid involved in the configuration of 3-OH. The H-3 is a broad triplet with a coupling constants 3.0 Hz (Table 1) implied that the *β* orientation of H-3 (thus *α* orientation of 3-OH), which was confirmed by analysis of the Newman projection. As depicted in Fig. 4, when the 3-OH occupied *α* orientation, nearly the same dihedral angles of H-2*β*/H-3 and H-2*α*/H-3 presented, thus the same of coupling constants between H-2*β*/H-3 and H-2*α*/H-3, corresponding to the triplet of H-3. Therefore, the structure of **2** was established as described in Fig. 1, and was given the trivial name irpeksolactin B.

Compound **3** was obtained as white, amorphous powder. The molecular formula of **3** was determined as $C_{31}H_{46}O_5$ on the basis of the sodium-adduct ion peak at *m/z* 521.3240 $[M + Na]^+$ (calcd for $C_{31}H_{46}O_5Na$, 521.3237) in the (+)-HRESIMS analysis. The absorption bands for hydroxy (3434 cm^{-1}), carbonyl (1706 cm^{-1}), and double bonds (1637 cm^{-1}) were observed in the IR spectrum. The ^{1}H and ^{13}C NMR spectroscopic data of **3** (Tables 1 and 3) resembled those of the known compound polyporenic acid C (Lai et al., 2016) with the exception of an additional oxymethine signal at δ_C 73.0 (C-15) and δ_H 4.12 (d, J = 7.0 Hz, H-15), which was substantiated by the ^{1}H–^{1}H COSY correlations of H-15/H-16 (Fig. 2). Furthermore, the ROESY correlations between H_3-18/H-15, and H_3-18/H-16 revealed that both 15-OH and 16-OH were *α* orientations. On the basis of the above information, the structure of compound **3** was established as shown in Fig. 1, and trivially named as irpeksolactin C.

Compound **4**, a white amorphous powder, was found to possess a molecular formula of $C_{31}H_{46}O_5$ based on the (+)-HRESIMS ion peak at *m/z* 499.3416 $[M + H]^+$ (calcd for $C_{31}H_{47}O_5$, 499.3418), suggesting eight degrees of unsaturation. The ^{1}H NMR data (Table 1) of **4** displayed characteristic signals of an eburicane skeleton same with those of compounds **2** and **3**: five methyl singlets at δ_H 1.22 (Me-18), 1.43 (Me-19), 1.39 (Me-28), 1.20 (Me-29) and 1.32 (Me-30), two isopropyl methyls at δ_H 1.00 (d, J = 6.0 Hz, Me-26) and 1.02 (d, J = 6.0 Hz, Me-27), one terminal olefinic methylene at δ_H 4.87 (s, H-31a) and 5.01 (s,

Table 3
^{13}C NMR spectroscopic data for compounds **1–10**.

No	1[a,d]	2[b,e]	3[b,d]	4[c,f]	5[c,e]	6[c,e]	7[b,e]	8[c,e]	9[b,e]	10[c,e]
1	26.8, CH_2	31.3, CH_2	36.6, CH_2	29.3, CH_2	37.1, CH_2	33.4, CH_2	35.4, CH_2	37.8, CH_2	37.2, CH_2	37.1, CH_2
2	30.7, CH_2	26.8, CH_2	34.8, CH_2	26.0, CH_2	28.4, CH_2	28.5, CH_2	35.9, CH_2	35.7, CH_2	28.6, CH_2	28.4, CH_2
3	79.2, CH	76.9, CH	216.6, C	74.4, CH	79.6, CH	74.6, CH	215.5, C	219.1, C	79.7, CH	79.6, CH
4	73.4, C	38.5, C	47.5, C	42.3, C	39.8, C	42.2, C	50.8, C	48.6, C	39.9, C	39.8, C
5	133.2, C	44.5, CH	50.5, CH	175.2, C	50.6, CH	88.1, C	89.4, C	52.3, CH	50.9, CH	50.7, CH
6	127.7, CH	24.1, CH_2	23.6, CH_2	126.6, CH	24.0, CH_2	133.9, CH	131.7, CH	24.6, CH_2	24.2, CH_2	24.1, CH_2
7	122.5, CH	123.1, CH	121.9, CH	200.9, C	122.9, CH	134.5, CH	135.5, CH	121.7, CH	122.2, CH	121.9, CH
8	144.5, C	142.3, C	140.3, C	53.6, CH	142.1, C	79.9, C	80.7, C	143.6, C	143.5, C	143.6, C
9	132.5, C	147.9, C	144.6, C	143.0, C	147.6, C	145.6, C	144.3, C	145.7, C	147.3, C	146.9, C
10	138.6, C	38.7, C	37.3, C	40.4, C	38.6, C	42.4, C	41.7, C	38.5, C	38.8, C	38.6, C
11	23.0, CH_2	116.4, CH	116.2, CH	118.5, CH	116.7, CH	121.0, CH	121.5, CH	118.3, CH	117.4, CH	117.7, CH
12	29.2, CH_2	37.5, CH_2	36.1, CH_2	35.7, CH_2	37.4, CH_2	36.6, CH_2	36.6, CH_2	36.8, CH_2	36.9, CH_2	37.2, CH_2
13	45.3, C	42.3, C	51.2, C	46.1, C	42.1, C	48.9, C	49.7, C	45.6, C	45.7, C	45.8, C
14	48.8, C	52.6, C	41.0, C	46.4, C	52.3, C	48.4, C	48.4, C	49.8, C	49.9, C	50.0, C
15	44.1, CH_2	74.0, CH	73.0, CH	48.4, CH_2	73.7, CH	42.0, CH_2	41.9, CH_2	44.3, CH_2	44.5, CH_2	44.1, CH_2
16	77.2, CH	76.1, CH	75.1, CH	76.6, CH	75.8, CH	77.0, CH	77.0, CH	77.3, CH	77.5, CH	76.0, CH
17	56.9, CH	56.6, CH	55.2, CH	56.6, CH	56.5, CH	57.2, CH	57.2, CH	57.7, CH	57.9, CH	54.1, CH
18	17.6, CH_3	18.1, CH_3	17.6, CH_3	16.7, CH_3	17.9, CH_3	18.4, CH_3	18.6, CH_3	17.7, CH_3	17.9, CH_3	18.2, CH_3
19	19.8, CH_3	23.4, CH_3	22.1, CH_3	30.6, CH_3	23.3, CH_3	29.0, CH_3	27.7, CH_3	22.4, CH_3	23.4, CH_3	23.2, CH_3
20	46.4, CH	48.8, CH	45.9, CH	48.6, CH	48.4, CH	48.2, CH	48.7, CH	49.2, CH	49.7, CH	49.6, CH
21	179.4, C	180.5, C	178.3, C	178.8, C	180.4, C	180.0, C	180.7, C	180.4, C	180.9, C	178.0, C
22	30.5, CH_2	33.5, CH_2	30.5, CH_2	31.6, CH_2	33.4, CH_2	34.3, CH_2	33.5, CH_2	30.7, CH_2	30.9, CH_2	23.8, CH_2
23	32.2, CH_2	32.0, CH_2	32.0, CH_2	33.2, CH_2	27.2, CH_2	27.3, CH_2	27.4, CH_2	30.5, CH_2	30.6, CH_2	21.9, CH_2
24	155.0, C	156.9, C	154.9, C	156.1, C	125.1, CH	125.2, CH	125.3, CH	80.0, CH	78.0, CH	85.9, CH
25	33.7, CH	35.2, CH	33.8, CH	34.1, CH	132.8, C	133.9, C	132.9, C	73.8, C	78.8, C	72.1, C
26	21.8, CH_3	22.4, CH_3	21.9, CH_3	21.9, CH_3	17.8, CH_3	17.9, CH_3	17.9, CH_3	24.9, CH_3	20.6, CH_3	25.4, CH_3
27	21.9, CH_3	22.5, CH_3	21.8, CH_3	22.0, CH_3	25.9, CH_3	26.1, CH_3	26.1, CH_3	25.6, CH_3	21.4, CH_3	25.4, CH_3
28	26.5, CH_3	29.1, CH_3	25.3, CH_3	27.5, CH_3	28.8, CH_3	24.2, CH_3	25.2, CH_3	25.8, CH_3	16.6, CH_3	28.8, CH_3
29	23.0, CH_3	23.5, CH_3	22.5, CH_3	30.4, CH_3	16.5, CH_3	19.5, CH_3	21.0, CH_3	22.9, CH_3	29.0, CH_3	16.5, CH_3
30	28.8, CH_3	18.2, CH_3	17.2, CH_3	18.6, CH_3	18.0, CH_3	20.0, CH_3	19.8, CH_3	26.4, CH_3	26.7, CH_3	26.9, CH_3
31	107.1, CH_2	107.5, CH_2	107.1, CH_2	107.1, CH_2						

[a] Recorded at 200 MHz.
[b] Recorded at 150 MHz.
[c] Recorded at 125 MHz.
[d] Recorded in $CDCl_3$.
[e] Recorded in CD_3OD.
[f] Recorded in C_5D_5N.

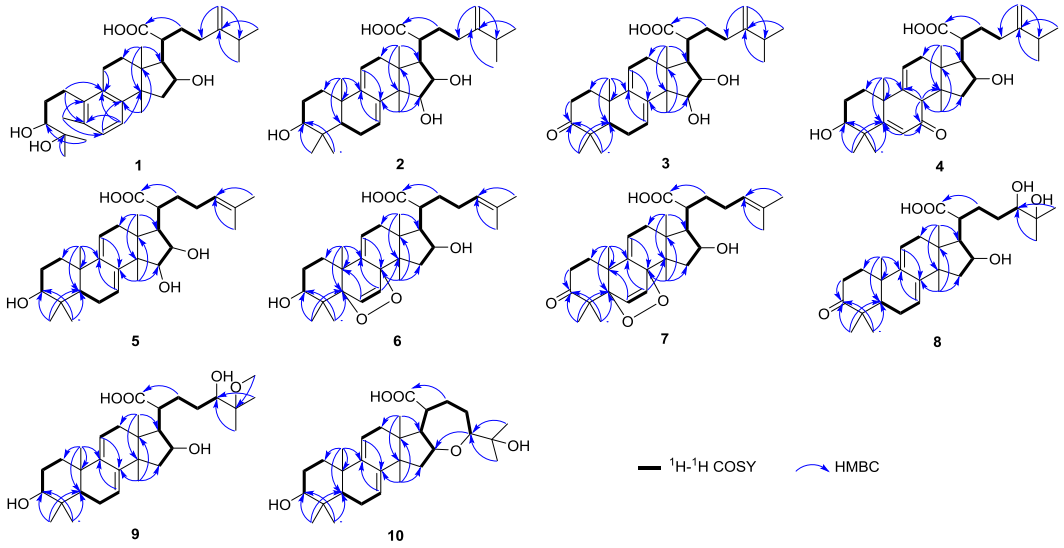

Fig. 2. Key ^{1}H−^{1}H COSY and HMBC correlations of compounds **1–10**.

H-31b). The ^{13}C NMR data (Table 3) were highly similar to those of poricoic acid ZH with only one exception (Wang et al., 2018). In poricoic acid ZH, the double bond located between C8−C9, while in compound **4**, it was located between C9−C11. The exception was confirmed by the ^{1}H−^{1}H COSY correlation between H-11 and H-12 (Fig. 2). The broad triplet of H-3 with small coupling constant (J = 3.5 Hz), and the diagnostic cross peaks between Me-18 and H-16 suggested that both 3-OH and 16-OH were *α* orientation (Figs. 2 and 3). Finally, the structure of **4** was established as shown in Fig. 1, and named trivially as irpeksolactin D.

Compound **5** possessed a molecular formula of $C_{30}H_{46}O_5$ as determined by the (+)-HRESIMS sodium-adduct ion peak at *m/z*

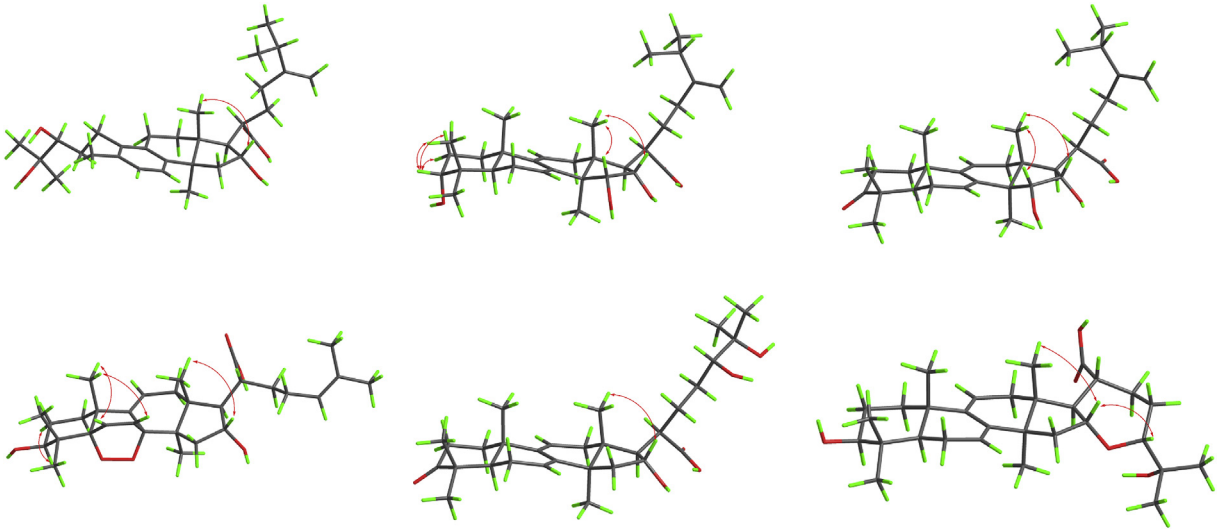

Fig. 3. Key ROESY correlations of compounds **1–10**.

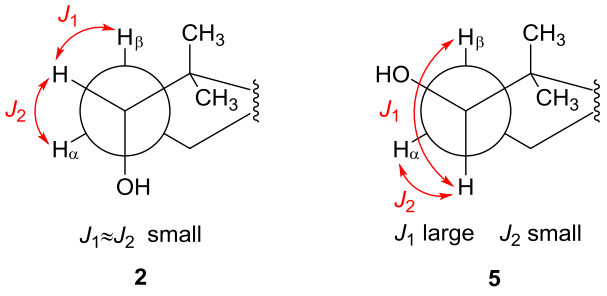

Fig. 4. Newman projections of C2−C3 of compounds **2** and **5**.

503.3250 [M + Na]$^+$ (calcd for 509.3237, $C_{30}H_{46}O_5Na$), indicating eight indices of hydrogen deficiency. The 1D NMR data (Tables 1 and 3), and HSQC spectra displayed typical signals of lanostane-type triterpenes: seven singlet methyls at δ_H 0.66 (Me-18), 0.99 (6H, Me-19 and Me-28), 1.60 (Me-26), 1.68 (Me-27), 0.87 (Me-29), 0.90 (Me-30), and four sp^3 quaternary carbons at δ_C 39.8 (C-4), 38.6 (C-10), 42.1 (C-13), and 52.3 (C-14). The 1D NMR data (Tables 1 and 3) exhibited high similarity with those of 15*α*-hydroxydehydrotumulosic acid (Akihisa et al., 2007). The structural discrepancy between **5** and 15*α*-hydroxydehydrotumulosic acid located at the terminal of the side chain by preliminary analysis of the 2D NMR spectra. In compound **5**, a double bond substituted at C-24 (25), while in 15*α*-hydroxydehydrotumulosic acid, the double bond located at C-24 (31), which was supported by HMBC correlations from H_3-26 and H_3-27 to C-24 and C-25 (Fig. 2). Thus, compound **5** was determined as shown in Fig. 1, and named as irpeksolactin E.

The molecular formula $C_{30}H_{44}O_6$ was assigned to **6** with nine indices of hydrogen deficiency by the (+)-HRSEIMS ion peak at *m/z* 523.3039 [M + Na]$^+$ (cacld for $C_{30}H_{44}O_6Na$, 523.3030). The ^{1}H NMR data (Table 2) showed seven methyl singlets at δ_H 0.85 (Me-18), 1.17 (Me-19), 1.60 (Me-26), 1.68 (Me-27), 1.07 (Me-28), 1.13 (Me-29), and 1.15 (Me-30), two oxymethine at δ_H 3.71 (dd, *J* = 11.0, 6.0 Hz, H-3) and 4.11 (t-like, *J* = 7.0 Hz, H-16), four olefinic protons at δ_H 6.54 (d, *J* = 9.0 Hz, H-6) and 6.80 (d, *J* = 9.0 Hz, H-7), 5.42 (d, *J* = 6.0 Hz, H-11), 5.14 (t, *J* = 6.4 Hz, H-24). A total of 30 carbon resonances were observed in ^{13}C NMR and DEPT spectra: carboxylic acid carbon at δ_C 180.0 (C-21), six olefinic carbons at δ_C 133.9 (C-6), 134.5 (C-7) and 145.6 (C-9), 121.0 (C-11), 125.2 (C-24), 133.9 (C-25), two oxymethines carbons at δ_C 74.6 (C-3) and 77.0 (C-16), and two oxygen bearing quaternary carbons at δ_C 88.1 (C-5) and 79.9 (C-8). The NMR data of **6** showed great similarities to those of 5*α*,8*α*-peroxydehydrotumulosic acid (Akihisa et al., 2007) except for the side chain at C-17. The reference compound 5*α*,8*α*-peroxydehydrotumulosic acid is an eburicane-type triterpene with a terminal double bond between C-24 and C-31, while compound **6** is a lanostane-type triterpene with a double bond between C-24 and C-25, which was substantiated by HMBC correlations from H_3-26 and H_3-27 to C-24 and C-25 (Fig. 2). The configuration of the 5,8-endoperoxy moiety, 16-OH, and 3-OH were ascertained by ROESY experiment (Fig. 3) to be same with those of 5*α*,8*α*-peroxydehydrotumulosic acid as *α*, *α*, *β* orientation, respectively. Therefore, compound **6** was established as irpeksolactin F (Fig. 1).

Compound **7**, white powder, has the molecular formula $C_{30}H_{42}O_6$ as deduced from the (+)-HRESIMS ion peak at *m/z* 521.2874 [M + Na]$^+$ (calcd for $C_{30}H_{42}O_6Na$, 521.2874), requiring 10 degrees of unsaturation. Comparing the ^{1}H and ^{13}C NMR data of **7** with those of **6** (Tables 2 and 3) clearly showed that the two compounds were similar in structure and stereochemistry. The C-3 of compound **7** was a carbonyl, while it was an oxymethine in compound **6**. The key HMBC correlations from H_3-28 (δ_H 1.42) and H_3-29 (δ_H 1.07) to C-3 (δ_C 215.5) supported this assignment (Fig. 2). Thus, compound **7** was named as irpeksolactin G and was depicted in Fig. 1.

Compound **8** gave a sodium-adduct ion peak at *m/z* 525.3175 [M + Na]$^+$ (calcd for $C_{30}H_{46}O_6Na$, 525.3187) in the (+)-HRESIMS analysis, appropriate for a molecular formula of $C_{30}H_{46}O_6$, indicating eight indices of hydrogen deficiency. The ^{1}H NMR data (Table 2) showed typical methyl signals of the lanostane skeleton: δ_H 0.66 (s, Me-18), 1.21 (s, Me-19), 1.12 (s, Me-26), 1.15 (s, Me-27), 1.07 (s, Me-28), 1.14 (s, Me-29), and 1.10 (s, Me-30). Totally 30 carbon signals were observed in the ^{13}C NMR and DEPT spectra (Tables 2 and 3), which were classified into seven methyls, seven methylenes, seven methines with two of which were oxymethines at δ_C 77.3 (C-16) and 80.0 (C-24), and nine quaternary carbons (a carboxylic acid group at δ_C 180.4 (C-21), a carbonyl at δ_C 219.1 (C-3), an oxygen-bearing one at δ_C 73.8 (C-25), and two olefinic ones at δ_C 143.6 (C-8) and 145.7 (C-9)). The 1D NMR data displayed similarity with those of 16*α*,25-dihydroxydehydroeburiconic acid (Akihisa et al., 2007) with the only exception of the substituted patterns of the side chain. For compound **8**, C-24 was substituted by a hydroxy group rather than forming a double bond between C-24 and C-31 in 16*α*,25-dihydroxydehydroeburiconic acid. This change was verified by HMBC correlations from H_3-26 and H_3-27 to C-24 (Fig. 2). 16-OH was assigned as *α* orientation by the ROESY correlations between H_3-18 (δ_H 0.66) and H-16 (δ_H 4.11). Due to the shortage of samples, the Mosher's method was unlikely to successfully determine the absolute configuration of C-24. However, the absolute configuration of C-24

should be empirically assigned by ^{13}C NMR chemical shifts. It was reported that C-24 gave resonance at δ_C 79.9–80.6 for *R* configuration, while it gave resonance at δ_C 77.0–78.2 for *S* configuration (Gulcemal et al., 2011). Based on the empirical rules, the C-24 of compound **8** was assigned as *R* configuration (δ_C 80.0). Therefore, compound **8** was named as irpeksolactin H (Fig. 1).

Compound **9** was obtained as a white, amorphous powder, and the molecular formula was established as $C_{31}H_{50}O_6$ on the basis of the (+)-HRESIMS sodium-adduct ion peak at *m/z* 541.3496 $[M + Na]^+$ (calcd for $C_{31}H_{50}O_6Na$, 541.3500). The 1D NMR spectra of **9** and **8** were highly similar to slight variations apparent at the C-3 and the presence of an additional methoxy in **9**. In compound **9**, C-3 and C-25 were substituted by a hydroxy group and methoxy group, respectively, while the counterpart carbons in compound **8** were substituted by a carbonyl and hydroxy group, respectively. This changes were supported by HMBC correlations from H_3-28 (δ_H 0.99) and H_3-29 (δ_H 0.88) to C-3 (δ_C 79.7), and the methoxy group (δ_H 3.20) to C-25 (δ_C 78.8). The 3-OH was assigned as β configuration by analysis of the coupling constants. However, the absolute configuration of C-24 was remained unassigned due to shortage of samples. Conclusively, the chemical structure of **9** was determined as shown in Fig. 1, and given the trivial name irpeksolactin I.

The ^1H and ^{13}C NMR data (Tables 2 and 3) of **10** showed similarity with those of compound **9**, indicating that **10** was a structural analogue of **9**. However, the molecular formula of **10**, which was established by HRESIMS as $C_{30}H_{46}O_5$ on the basis of the ion peak at *m/z* 487.3418 $[M + H]^+$ (calcd for $C_{30}H_{47}O_5$, 487.3418), requiring eight degrees of unsaturation. The evidence revealed that the presence of one more ring in **10** than that of **9**. Analysis of the HMBC spectrum of **10** demonstrated that the additional ring was formed by an ether bond between C-16 and C-24 as supported by the HMBC correlation from H-16 (δ_H 4.18) to C-24 (δ_C 85.9) (Fig. 2). The 16-ether bond and C-24 were determined as β and *R* configuration, respectively, by the key ROESY correlations between H_3-18/H-16/H-24 (Fig. 3). Therefore, compound **10** was established as shown in Fig. 1, and named as irpeksolactin J.

Eighteen known compounds were accompanied in this research, they are asiatic acid (**11**) (He et al., 2010), 15α-hydroxydehydrotumulosic acid (**12**) (Akihisa et al., 2007), polyporenic acid C (**13**) (Lai et al., 2016), 24-methylene-lanosta-7,9 (11)-diene-3-one (**14**) (Lan et al., 2007), 29-hydroxypolyporenic acid C (**15**) (Zheng and Yang, 2008), 6α-hydroxypolyporenic acid C (**16**) (Pinhey et al., 1971), dehydrosulphurenic acid (**17**) (Yang et al., 1996), polycarpol (**18**) (Ngantchou et al., 2009), dehydrotrametenonic acid (**19**) (Akihisa et al., 2004), 3-oxo-6,16α-dihydroxylanosta-7,9(11),24(31)-trien-21-oic acid (**20**) (Wu et al., 2016), ganoderol A (**21**) (Hajjaj et al., 2005), 13α,14β,17α-lanosta-7,9,24-triene-3β,16α-diol (**22**) (Venkatraman et al., 1994), 3α-hydroxy-24-methylene-23-oxolanost-8-en-26-carboxylic acid (**23**) (Popova et al., 2009), 3α-carboxyacetoxyquercinic acid (**24**) (Rosecke and Konig, 2000), inonotusane C (**25**) (Zhao et al., 2015), daedalol C (**26**) (Sorribas et al., 2011), ganodermanondiol (**27**) (Huang et al., 2017), hexatenuins B (**28**) (Umeyama et al., 2014) (Fig. S1. Supplementary material).

2.2. Biological activities

All the undescribed compounds were tested for their cytotoxicity against the five human cancer cell lines, the HL-60 (ATCC CCL-240) human myeloid leukemia cell line, the SMMC-7721 human hepatocellular carcinoma cell line, the A549 (ATCC CCL-185) lung cancer cell line, the MCF-7 (ATCC HTB-22) breast cancer cell line, and the SW-480 (ATCC CCL-228) human colon cancer cell line. However, only compound **10** displayed selective and weak cytotoxicity against the human lung cancer cell line A549 and the human hepatocellular carcinoma cell line SMMC-7721 with inhibition rates of 54.6%, and 50.0% at the concentration of 40 μM, respectively, while it was devoid of activity against the other three cancer cell lines, the human myeloid leukemia cell line HL-60, the breast cancer cell line MCF-7, and the human colon cancer cell line SW-480.

3. Conclusions

In conclusion, twenty-eight triterpenoid, including ten previously undescribed ones (**1–10**), were identified from the fruiting bodies of *I. lacteus*. Amongst them compound **10** displayed weak cytotoxicity against the human lung cancer cell line A549 and the human hepatocellular carcinoma cell line SMMC-7721. Our findings has expanded the natural sources of fungal triterpenoids, and has casted light on the profile of specialised metabolites of *I. lacteus*, which provides evidences for the downstream research of this fungus.

4. Experimental

4.1. General experimental procedures

Optical rotations were obtained on a JASCO P-1020 digital polarimeter (Horiba, Ltd., Kyoto, Japan). UV spectra were recorded on a Shimadzu UV-2401PC UV–visible recording spectrophotometer (Shimadzu Corporation, Kyoto, Japan). IR spectra were obtained using a Bruker Tensor 27 FT-IR spectrometer (Bruker Optics, Inc., Billerica, MA) with KBr pellets. 1D and 2D NMR spectra were obtained on Bruker Avance III 600 MHz or Ascend 800 MHz spectrometers (Bruker Corporation, Karlsruhe, Germany). HRESIMS were recorded on an Agilent 6200 Q-TOF MS system (Agilent Technologies, Santa Clara, CA, USA). HREIMS were recorded on a Waters Auto-Spec Premier P776 mass spectrometer (Waters, Milford, MA, USA). Sephadex LH-20 (Amersham Biosciences, Uppsala, Sweden) and silica gel (Qingdao Haiyang Chemical Co., Ltd., Qingdao, China) were used for column chromatography (CC). Medium pressure liquid chromatography (MPLC) was performed on a Büchi Sepacore System equipped with pump manager C-615, pump modules C-605 and fraction collector C-660 (Büchi Labortechnik AG, Flawil, Switzerland), and columns packed with Chromatorex C-18 (dimension 450 mm × i.d. 14 mm, particle size: 40–75 μm, flow rate 40 mL min^{-1}, Fuji Silysia Chemical Ltd., Kasugai, Japan). Preparative high performance liquid chromatography (prep. HPLC) were performed on an Agilent 1260 liquid chromatography system equipped with a Zorbax SB-C18 column (particle size 5 μm, dimension 150 mm × i.d. 9.4 mm, flow rate 7 mL min^{-1}, Agilent Technologies), and a Zorbax SB C-8 column (particle size 5 μm, dimension 250 mm × i.d. 9.4 mm, flow rate 5 mL min^{-1}, Agilent Technologies).

Five human cancer cell lines were used to evaluate the cytotoxicities of these isolated compounds: the HL-60 (ATCC CCL-240) human myeloid leukemia; SMMC-7721 human hepatocellular carcinoma; A-549 (ATCC CCL-185) lung cancer; MCF-7 (ATCC HTB-22) breast cancer; SW-480 (ATCC CCL-228) human colon cancer. The cell line SMMC-7721 was bought from China Infrastructure of Cell Line Resources (Beijing, China), and others were bought from American Type Culture Collection (ATCC, Manassas, VA). Roswell Park Memorial Institute (RPMI) 1640 medium (HyClone, GL Healthcare, IL, USA) containing 10% fetal bovine serum (HyClone, GL Healthcare, Australia) were used for cancer cell lines. 3-(4,5-dimethylthiazol-2-yl)-2,5-diphenyltetrazolium bromide (MTT) and cisplatin were bought from Sigma, St. Louis, MO. Corning® Costar® 96-Well Cell Culture Plates (Corning Incorporated, NY, USA) were used to culture the cell lines. EnVision® 2104 Multilabel Plate Reader (PerkinElmer Inc., Waltham, MA, U.S.) was used to measure the optical density at 595 nm in cytotoxicity assays.

4.2. Fungal material

Fruiting bodies of the crust fungus *Irpex lacteus* (Fr.) Fr. (Phanerochaetaceae) were collected on an identified fallen tree in the

Xishuangbanna Wangtianshu scenic area, Yunnan Province in July 2014 by Dr. Zhenghui Li. The fungus was identified by Prof. Yucheng Dai (Beijing Forestry University). A voucher specimen of *I. lacteus* was deposited at the Mushroom Bioactive Natural Products Research Group in South-Central University of Nationalities (No. HFG 201407).

4.3. Extraction and isolation

The powder of dry fruiting bodies of *Irpex lacteus* (1.47 kg) was macerated five times with 95% EtOH at room temperature. The extract was evaporated under reduced pressure and then partitioned between EtOAc and water for five times to give an EtOAc layer (93 g). The crude extract was eluted on MPLC with a stepwise gradient of MeOH/H_2O (20–100%) affording eight fractions (A–H).

Fraction B was separated by Sephadex LH-20 (MeOH) to give two major subfractions (B1−B2). Subfraction B1 was separated into 8 fractions (B1a–B1h) by prep-HPLC (MeCN/H_2O: 30–40%, 7 mL/min, 20 min). Subfraction B1c was purified on prep-HPLC (MeCN/H_2O: 35–43%, 5 mL/min, 20min) to yield compounds **8** (2.3 mg, t_R = 12.7 min) and **9** (2.4 mg, t_R = 13.6 min). Likewise, compound **10** (2.3 mg. MeCN/H_2O: 38–42%, 5 mL/min, 20 min, t_R = 17.9 min) by prep-HPLC from B1f.

Subfraction B2 was applied to silica gel column chromatography eluted with petroleum ether/acetone (5:1 to 1:1 (v/v)) to give seven subfractions (B2a–B2g). Subfraction B2d and B2e were purified on prep-HPLC (MeCN/H_2O: 38–43%, 7 mL/min, 20min) to obtain compounds **6** (2.6 mg, t_R = 12.3 min) and **7** (1.9 mg, t_R = 14.8 min).

Fraction C was subjected to silica gel column chromatography ($CHCl_3$/MeOH from 10:1 to 0:1) affording four subfractions (C1−C4). Subfraction C1 and C2 were combined and divided into five subfractions (C1a–C1e) by Sephadex LH-20 column chromatography, eluting with MeOH. Subfraction C1c was chromatographed over a silica gel column ($CHCl_3$/MeOH from 70:1 to 1:1) to give seven subfractions (C1c1–C1c7). Subfraction C1c6 was purified on prep-HPLC (MeCN/H_2O: 40–45%, 7 mL/min, 20 min) to afford compound **4** (2.3 mg, t_R = 13.1 min). Subfraction C1e was again fractionated by silica column chromatography, eluting with $CHCl_3$/MeOH (70:1 to 10:1), and to gain seven subfractions (C1e1–C1e7). Subfraction C1e3 further separated by prep-HPLC (MeCN/H_2O: 40–60%, 7 mL/min, 20 min) to afford compound **5** (2.0 mg, t_R = 14.0 min).

Fraction D was eluted on Sephadex LH-20 with MeOH to receive nine fractions (D1–D9). Fraction D3 was purified by prep-HPLC eluting with gradient solvent system from 40% to 65% MeCN/H_2O over 25 min to afford compound **1** (1.3 mg, t_R = 9.5 min). Subfraction D7 was subject to silica gel column chromatography, eluting with step gradient of petroleum ether and acetone (7:1 to 1:1), and five subfractions (D7a–D7e) was collected. Subfraction D7a was purified by prep-HPLC on C18 column using MeCN/H_2O (30–50%, 7 mL/min, 25 min) to yield compound **3** (2.4 mg, t_R = 20.5 min).

Fraction F was subjected to passage over a silica gel column ($CHCl_3$/MeOH, 40:1 to 1:1) to furnish seven fractions (F1−F7). Fraction F4 was fractionated into five subfractions (F4a–F4e) by Sephadex LH-20, eluting with $CHCl_3$/MeOH (1:1). Subfraction F4e was separated using silica gel column chromatography ($CHCl_3$/MeOH, 100:1 to 10:1) to afford eight subfractions (F4e1–F4e8). Subfraction F4e6 and F4e7 were combined and purified employing prep-HPLC (MeCN/H_2O: 40–57%, 7 mL/min, 20 min). Compound **2** (1.8 mg, t_R = 11.6 min) was isolated upon purification of subfraction F4e6a by prep-HPLC on C-8 column (MeCN/H_2O, 54% isocratic, 5 mL/min, 20 min).

4.4. Spectroscopic data of compounds

4.4.1. Irpeksolactin A (1)

White, amorphous powder; [α]24 D +9.40 (*c* 0.10, MeOH); UV (MeOH) λ_{max} (log ε) 202.8 (4.38), 215.6 (3.95); ^{1}H NMR (800 MHz, $CDCl_3$) and ^{13}C NMR (200 MHz, $CDCl_3$) data: Tables 1 and 3; HRESIMS *m/z* 523.3398 $[M + Na]^+$ (calcd for $C_{31}H_{48}O_5Na$, 523.3394).

4.4.2. Irpeksolactin B (2)

White, amorphous powder; [α]24 D +25.15 (*c* 0.18, MeOH); ^{1}H NMR (600 MHz, CD_3OD) and ^{13}C NMR (150 MHz, CD_3OD) data: Tables 1 and 3; HRESIMS *m/z* 501.3572 $[M + H]^+$ (calcd for $C_{31}H_{49}O_5$, 501.3575).

4.4.3. Irpeksolactin C (3)

White, amorphous powder; [α]24 D +18.07 (*c* 0.05, MeOH); UV (MeOH) λ_{max} (log ε) 200.0 (3.78), 238.6 (4.09), 242.0 (4.11) and 250.0 (3.97); IR (KBr) ν_{max} 3434, 2964, 2930 1705, 1383 cm^{-1}; ^{1}H NMR (600 MHz, $CDCl_3$) and ^{13}C NMR (150 MHz, $CDCl_3$) data: Tables 1 and 3; HRESIMS *m/z* 521.3240 $[M + Na]^+$ (calcd for $C_{31}H_{46}O_5Na$, 521.3237).

4.4.4. Irpeksolactin D (4)

White, amorphous powder; [α]24 D −48.53 (*c* 0.05, MeOH); ^{1}H NMR (500 MHz, C_5D_5N) and ^{13}C NMR (125 MHz, C_5D_5N) data: Tables 1 and 3; HRESIMS *m/z* 499.3416 $[M + H]^+$ (calcd for $C_{31}H_{47}O_5$, 499.3418).

4.4.5. Irpeksolactin E (5)

White, amorphous powder; [α]24 D +46.10 (*c* 0.14, MeOH); ^{1}H NMR (500 MHz, CD_3OD) and ^{13}C NMR (125 MHz, CD_3OD) data: Tables 1 and 3; HRESIMS *m/z* 503.3250 $[M + Na]^+$ (calcd for $C_{30}H_{46}O_5Na$, 509.3237).

4.4.6. Irpeksolactin F (6)

White, amorphous powder; [α]24 D +73.42 (*c* 0.24, MeOH); ^{1}H NMR (500 MHz, CD_3OD) and ^{13}C NMR (125 MHz, CD_3OD) data: Tables 2 and 3; HRESIMS *m/z* 523.3039 $[M + Na]^+$ (cacld for $C_{30}H_{44}O_6Na$, 523.3030).

4.4.7. Irpeksolactin G (7)

White, amorphous powder; [α]24 D +68.86 (*c* 0.07, MeOH); ^{1}H NMR (600 MHz, CD_3OD) and ^{13}C NMR (150 MHz, CD_3OD) data: Tables 2 and 3; HRESIMS *m/z* 521.2874 $[M + Na]^+$ (calcd for $C_{30}H_{42}O_6Na$, 521.2874).

4.4.8. Irpeksolactin H (8)

White, amorphous powder; [α]24 D −17.67 (*c* 0.08, MeOH); ^{1}H NMR (500 MHz, CD_3OD) and ^{13}C NMR (125 MHz, CD_3OD) data: Tables 2 and 3; HRESIMS *m/z* 525.3175 $[M + Na]^+$ (calcd for $C_{30}H_{46}O_6Na$, 525.3187).

4.4.9. Irpeksolactin I (9)

White, amorphous powder; [α]24 D +17.07 (*c* 0.05, MeOH); ^{1}H NMR (600 MHz, CD_3OD) and ^{13}C NMR (150 MHz, CD_3OD) data: Tables 2 and 3; HRESIMS *m/z* 541.3496 $[M + Na]^+$ (calcd for $C_{31}H_{50}O_6Na$, 541.3500).

4.4.10. Irpeksolactin J (10)

White, amorphous powder; [α]24 D +16.93 (*c* 0.05, MeOH); ^{1}H NMR (500 MHz, CD_3OD) and ^{13}C NMR (125 MHz, CD_3OD) data: Tables 2 and 3; HRESIMS *m/z* 487.3418 $[M + H]^+$ (calcd for $C_{30}H_{47}O_5$, 487.3418).

4.5. Cytotoxicity against five human cancer cell lines

All cells were cultured in RPMI-1640 medium containing 10% fetal bovine serum (FBS) and maintained at 37 °C under 5% CO_2 in a humidified atmosphere. Colorimetric measurements of the amount of insoluble formazan which produced in living cells based on the reduction of 3-(4,5-dimethylthiazol-2-yl)-2,5-diphenyltetrazolium bromide (MTT) was used to assess cell viability. In brief, each well of a 96-well cell culture plate was seeded with 100 μL of adherent cells and kept for 12 h

for adherence, and then added with test compounds (solved in DMSO), however, suspended cells were seeded before added with test compounds with both the same density of 1×10^5 cells/mL every 100 μL of culture medium. After test compounds addition (40 μM), each cancer cell line was incubated for 48 h in triplicates. Cisplatin was used as positive control for every cancer cell line. After the incubation, each well was added with MTT (100 μg) and continued to incubate for 4 h at 37 °C. After removed the 100-μL culture medium, the cells were lysed with 20% SDS-50% DMF (100 μL). The remained lysates were subjected to measure the optical density at 595 nm with a 96-well microtiter plate reader.

Acknowledgements

This work was financially supported by National Natural Science Foundation of China (No. 81561148013, 81773590), National Key Technologies R&D Program of China (2017YFC1704007), and the State Key Laboratory of Phytochemistry and Plant Resources in West China (No. P2017-KF01). We thank Analytical & Measuring Center, School of Pharmaceutical Sciences, South-Central University for Nationalities for MS and NMR spectra tests. The computational work was supported by the Supercomputing Center of the Chinese Academy of Sciences in Beijing.

Appendix A. Supplementary data

Supplementary data to this article can be found online at https://doi.org/10.1016/j.phytochem.2019.02.017.

References

Akihisa, T., Mizushina, Y., Ukiya, M., Oshikubo, M., Kondo, S., Kimura, Y., Suzuki, T., Tai, T., 2004. Dehydrotrametenonic acid and dehydroeburiconic acid from *Poria cocos* and their inhibitory effects on eukaryotic DNA polymerase α and β. Biosci. Biotechnol. Biochem. 68, 448–450.

Akihisa, T., Nakamura, Y., Tokuda, H., Uchiyama, E., Suzuki, T., Kimura, Y., Uchikura, K., Nishino, H., 2007. Triterpene acids from *Poria cocos* and their anti-tumor-promoting effects. J. Nat. Prod. 70, 948–953.

Cajthaml, T., Erbanova, P., Kollmann, A., Novotny, C., Sasek, V., Mougin, C., 2008. Degradation of PAHs by ligninolytic enzymes of *Irpex lacteus*. Folia Microbiol. 53, 289–294.

Ding, J.H., Feng, T., Cui, B.K., Wei, K., Li, Z.H., Liu, J.K., 2013. Novel sesquiterpenoids from cultures of the basidiomycete *Irpex lacteus*. Tetrahedron Lett. 54, 2651–2654.

Dong, X.M., Song, X.H., Liu, K.B., Dong, C.H., 2017. Prospect and current research status of medicinal fungus *Irpex lacteus*. Mycosystema 36, 28–34.

Gulcemal, D., Alankus-Caliskan, O., Perrone, A., Ozgokce, F., Piacente, S., Bedir, E., 2011. Cycloartane glycosides from *Astragalus aureus*. Phytochemistry 72, 761–768.

Hajjaj, H., Macé, C., Roberts, M., Niederberger, P., Fay, L.B., 2005. Effect of 26-oxygenosterols from *Ganoderma lucidum* and their activity as cholesterol synthesis inhibitors. Appl. Environ. Microbiol. 71, 3653–3658.

Hayashi, M., Wada, K., Munakata, K., 1981. New nematocidal metabolites from a fungus, *Irpex lacteus*. Agric. Biol. Chem. 45, 1527–1529.

He, W.N., Dai, J.G., Ye, M., Wu, L.J., Guo, D.A., 2010. Microbial transformation of asiatic acid by *Alternaria longipes*. J. Asian Nat. Prod. Res. 12, 760–764.

Huang, S.Z., Ma, Q.Y., Kong, F.D., Guo, Z.K., Cai, C.H., Hu, L.L., Zhou, L.M., Wang, Q., Dai, H.F., Mei, W.L., Zhao, Y.X., 2017. Lanostane-type triterpenoids from the fruiting body of *Ganoderma calidophilum*. Phytochemistry 143, 104–110.

Lai, K.H., Lu, M.C., Du, Y.C., El-Shazly, M., Wu, T.Y., Hsu, Y.M., Henz, A., Yang, J.C., Backlund, A., Chang, F.R., Wu, Y.C., 2016. Cytotoxic lanostanoids from *Poria cocos*. J. Nat. Prod. 79, 2805–2813.

Lan, Y.H., Wang, H.Y., Wu, C.C., Chen, S.L., Chang, C.L., Chang, F.R., Wu, Y.C., 2007. New constituents from stems of *Artabotrys uncinatus*. Chem. Pharm. Bull. 55, 1597–1599.

Ngantchou, I., Nkwengoua, E., Nganso, Y., Nyasse, B., Denier, C., Hannaert, V., Schneider, B., 2009. Antitrypanosomal activity of polycarpol from *Piptostigma preussi* (Annonaceae). Fitoterapia 80, 188–191.

Pinhey, J., Ralph, B., Simes, J., Wootton, M., 1971. Extractives of fungi. II. The constituents of Trametes feei . 6α-Hydroxypolyporenic acid C. Aust. J. Chem. 24, 609–619.

Popova, M., Trusheva, B., Gyosheva, M., Tsvetkova, I., Bankova, V., 2009. Antibacterial triterpenes from the threatened wood-decay fungus *Fomitopsis rosea*. Fitoterapia 80, 263–266.

Rosecke, J., Konig, W.A., 2000. Constituents of the fungi *Daedalea quercina* and *Daedaleopsis confragosa* var. *tricolor*. Phytochemistry 54, 757–762.

Sorribas, A., Jimenez, J.I., Yoshida, W.Y., Williams, P.G., 2011. Daedalols A-C, fungal-derived BACE1 inhibitors. Bioorg. Med. Chem. 19, 6581–6586.

Tang, Y., Zhao, Z.Z., Li, Z.H., Feng, T., Chen, H.P., Liu, J.K., 2018a. Irpexoates A–D, four triterpenoids with malonyl modifications from the fruiting bodies of the medicinal fungus *Irpex lacteus*. Nat. Prod. Bioprospect. 8, 171–176.

Tang, Y., Zhao, Z.Z., Yao, J.N., Feng, T., Li, Z.H., Chen, H.P., Liu, J.K., 2018b. Irpeksins A–E, 1,10-*seco*-eburicane-type triterpenoids from the medicinal fungus *Irpex lacteus* and their anti-NO activity. J. Nat. Prod. 81, 2163–2168.

Umeyama, A., Ohta, C., Shino, Y., Okada, M., Nakamura, Y., Hamagaki, T., Imagawa, H., Tanaka, M., Ishiyama, A., Iwatsuki, M., Otoguro, K., Omura, S., Hashimoto, T., 2014. Three lanostane triterpenoids with antitrypanosomal activity from the fruiting body of *Hexagonia tenuis*. Tetrahedron 70, 8312–8315.

Venkatraman, G., Thombare, P.S., Sabata, B.K., 1994. A tetracyclic triterpenoid from *Garuga pinnata*. Phytochemistry 36, 417–419.

Wang, M., Chen, D.Q., Chen, L., Liu, D., Zhao, H., Zhang, Z.H., Vaziri, N.D., Guo, Y., Zhao, Y.Y., Cao, G., 2018. Novel RAS inhibitors poricoic acid ZG and poricoic acid ZH attenuate renal fibrosis via a wnt/β-catenin pathway and targeted phosphorylation of Smad3 signaling. J. Agric. Food Chem. 66, 1828–1842.

Wu, L.F., Wang, K.F., Mao, X., Liang, W.Y., Chen, W.J., Li, S., Qi, Q., Cui, Y.P., Zhang, L.Z., 2016. Screening and analysis of the potential bioactive components of Poria cocos (Schw.) Wolf by HPLC and HPLC-MSn with the aid of chemometrics. Molecules 21.

Yang, S.W., Shen, Y.C., Chen, C.H., 1996. Steroids and triterpenoids of *Antrodia cinnamomea* - a fungus parasitic on *Cinnamomum micranthum*. Phytochemistry 41, 1389–1392.

Yao, M.W., Li, W.M., Duan, Z.H., Zhang, Y.L., Jia, R., 2017. Genome sequence of the white-rot fungus *Irpex lacteus* F17, a type strain of lignin degrader fungus. Stand. Genomic Sci. 12.

Yoshikawa, K., Kouso, K., Takahashi, J., Matsuda, A., Okazoe, M., Umeyama, A., Arihara, S., 2005. Cytotoxic constituents of the fruit body of *Daedalea dickisii*. J. Nat. Prod. 68, 911–914.

Zhao, F.Q., Mai, Q.Q., Ma, J.H., Xu, M., Wang, X., Cui, T.T., Qiu, F., Han, G., 2015. Triterpenoids from *Inonotus obliquus* and their antitumor activities. Fitoterapia 101, 34–40.

Zheng, Y., Yang, X.W., 2008. Two new lanostane triterpenoids from *Poria cocos*. J. Asian Nat. Prod. Res. 10, 289–292.